Supplementary Material (ESI) for Journal of Materials Chemistry

Supporting Information

Functionalization of MCM-41 and SBA-1 with Titanium(IV) (Silyl)Amides

*Thomas Deschner,[a] Bjørn-Tore Lønstad,[a] Markus Widenmeyer,[b] and Reiner Anwander[a,b]**

[a]Kjemisk Institutt, Universitetet i Bergen, Allégaten 41, 5007 Bergen, Norway; [b]Institut für Anorganische Chemie, Eberhard Karls Universität Tübingen, Auf der Morgenstelle 18, 72076 Tübingen, Germany

Synthesis of the Periodic Mesoporous Silica Materials

MCM-41. CTMABr (4.27 g, 11.71 mmol) and 5.51 g $C_{16\text{-}3\text{-}1}$ (10.39 mmol) were combined with distilled water (280.76 g, 15.60 mol) and 23.65 g TMAOH solution (64.88 mmol) and stirred for 30 minutes until a homogenous solution was achieved. Then TEOS (27.04 g, 129.78 mmol) was added and the resulting solution stirred for 40 minutes. The material was filtrated, re-suspended in 350 mL of distilled water, transferred into a Teflon autoclave and treated for 6 D at 100 °C. The solid product was recovered by filtration and dried at ambient temperature. The as-synthesized material was calcined at 540 °C (air, 5 h) and dehydrated in vacuo (270 °C, 10^{-4} Torr, 8 h). The molar composition of the synthesis gel was 0.08:0.08: 120: 0.5:1 CTMABr:$C_{16\text{-}3\text{-}1}$:H_2O:TMAOH:TEOS.

SBA-1. C_{18}TEABr (5.70 g, 13.08 mmol), concentrated HCl (37 wt%, 362.9 g, 3.18 mol) and distilled water (598.5 g, 33.23 mol) were combined, and the resulting mixture vigorously stirred until a homogeneous solution formed (ca. 30 min). The solution was cooled to 0 °C in an ice bath and 13.68 g (65.67 mmol) of TEOS slowly added. Stirring was continued for 4 h at 0 °C, and then the reaction mixture heated in a polypropylene bottle to 100 °C and maintained there for 1 h without stirring. The solid product was recovered by filtration (without washing) and dried at ambient temperature. The as-synthesized material was calcined at 540 °C (air, 5 h) and dehydrated in vacuo (270 °C, 10^{-4} Torr, 8 h). The molar composition of the synthesis gel was 1:5:280:3500 C_{18}TEABr:TEOS:HCl:H_2O.

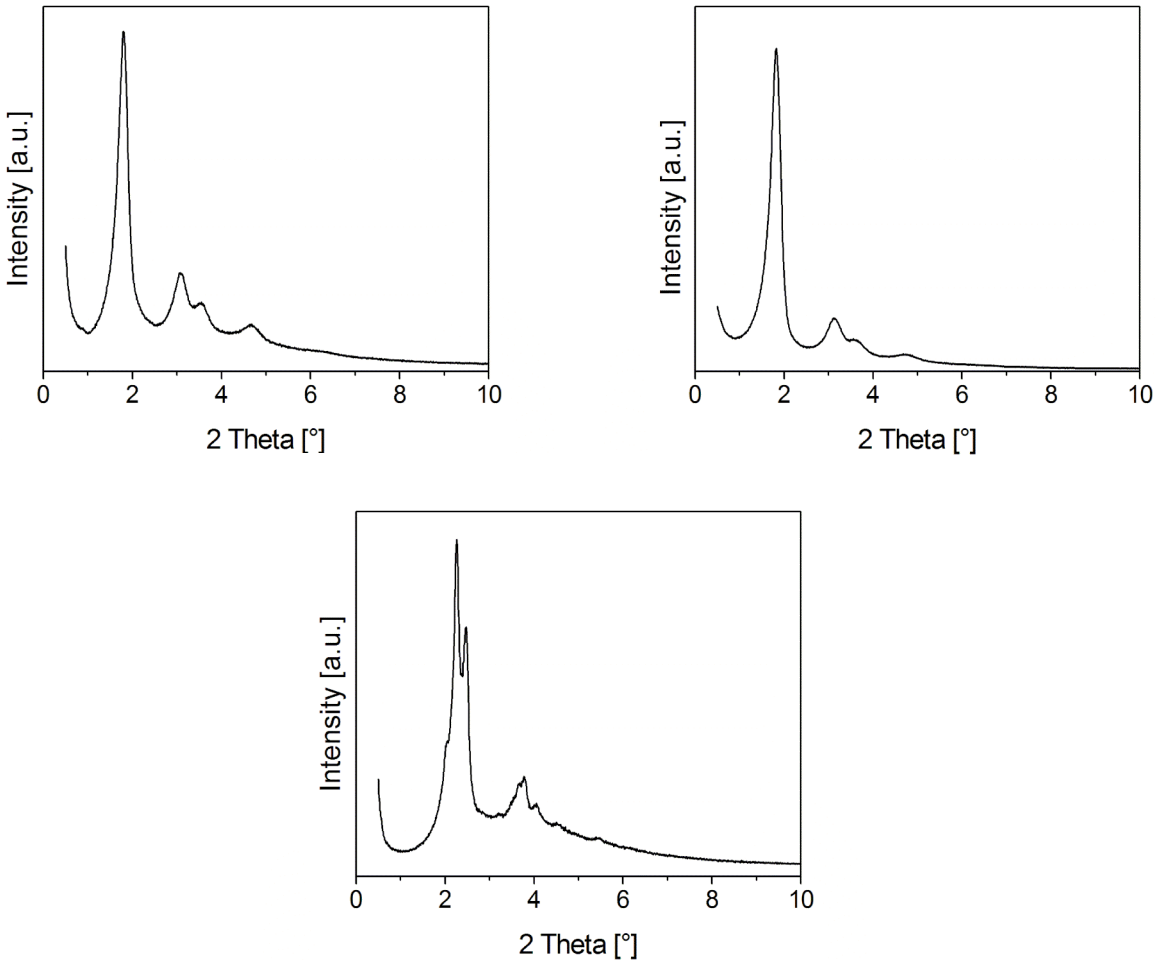

Figure S1. Powder XRD patterns of the parent materials: MCM-41 (**1**) (upper left), MCM-41 (**2**) (upper right), and SBA-1 (**3**) (bottom).

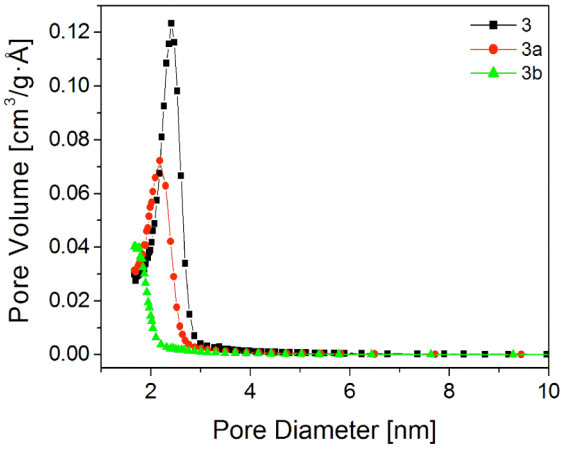

Figure S2. BJH pore size distribution of SBA-1 **(3)** (■), $SiMePh_2$@ SBA-1 **(3a)** (●) and $Ti(NMe_2)_4$@$SiMePh_2$@SBA-1 **(3b)** (▲).

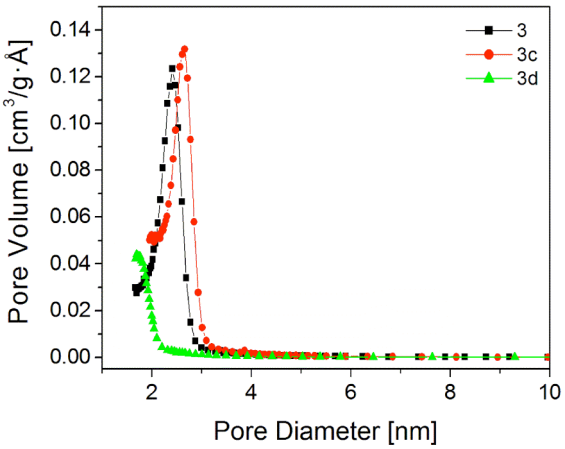

Figure S3. BJH pore size distribution of SBA-1 **(3)** (■), $Mg[N(SiHMe_2)_2]_2$@SBA-1 **(3c)** (●) and $Ti(NMe_2)_4$@ $Mg[N(SiHMe_2)_2]_2$@SBA-1 **(3d)** (▲).

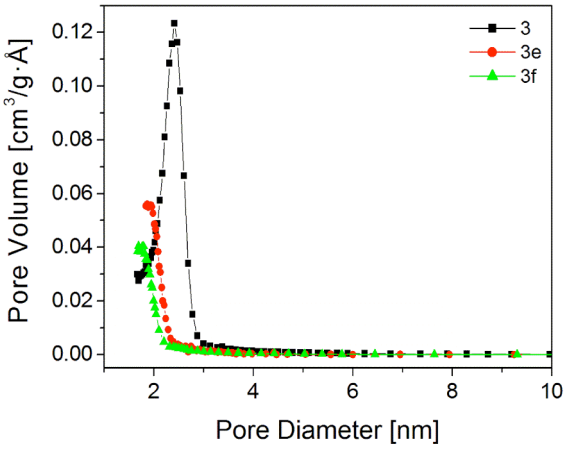

Figure S4. BJH pore size distribution of SBA-1 **(3)** (■), $Ti(NMe_2)_4$@SBA-1 **(3e)** (●) and (*R*-H_2BINOL)@$Ti(NMe_2)_4$@SBA-1 **(3f)** (▲).

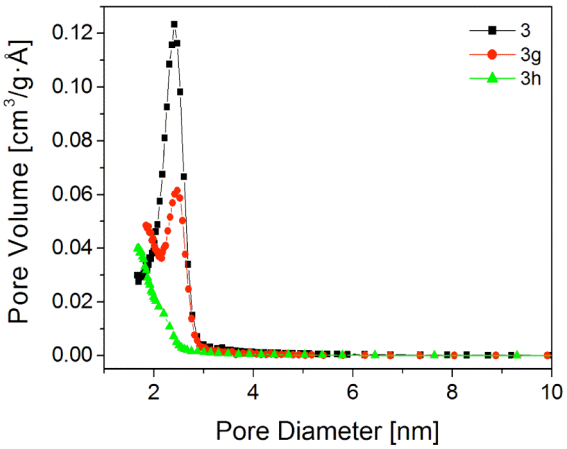

Figure S5. BJH pore size distribution of SBA-1 **(3)** (■),$Ti(NMe_2)_3[N(SiHMe_2)_2]$@ SBA-1 **(3g)** (●) and $Ti(NMe_2)_3[N(SiHMe_2)_2]$@SBA-1 **(3h)** (▲).

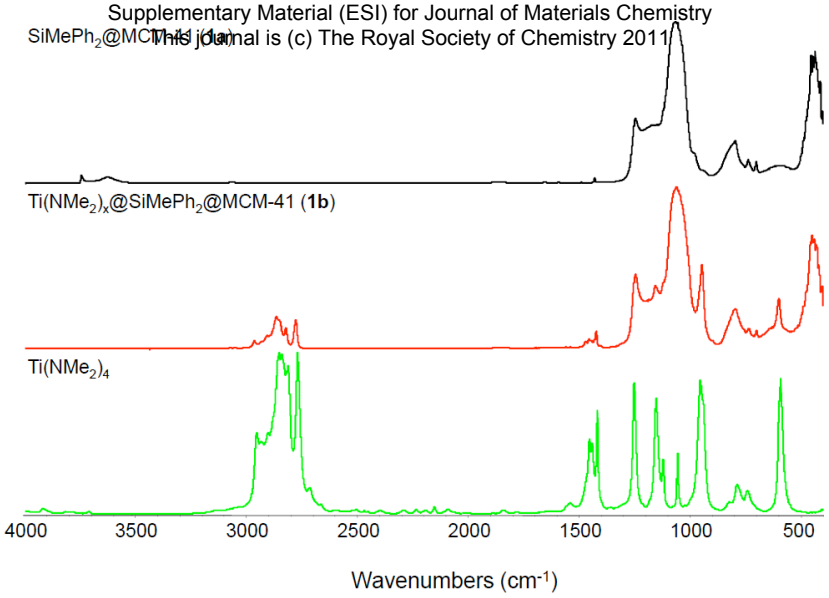

Figure S6. IR spectra (DRIFT) of the hybrid materials $SiMePh_2$@MCM-41 (**1a**) and $Ti(NMe_2)_4$@$SiMePh_2$@MCM-41 (**1b**) and precursor $Ti(NMe_2)_4$ in the range of 400-4000 cm^{-1}.

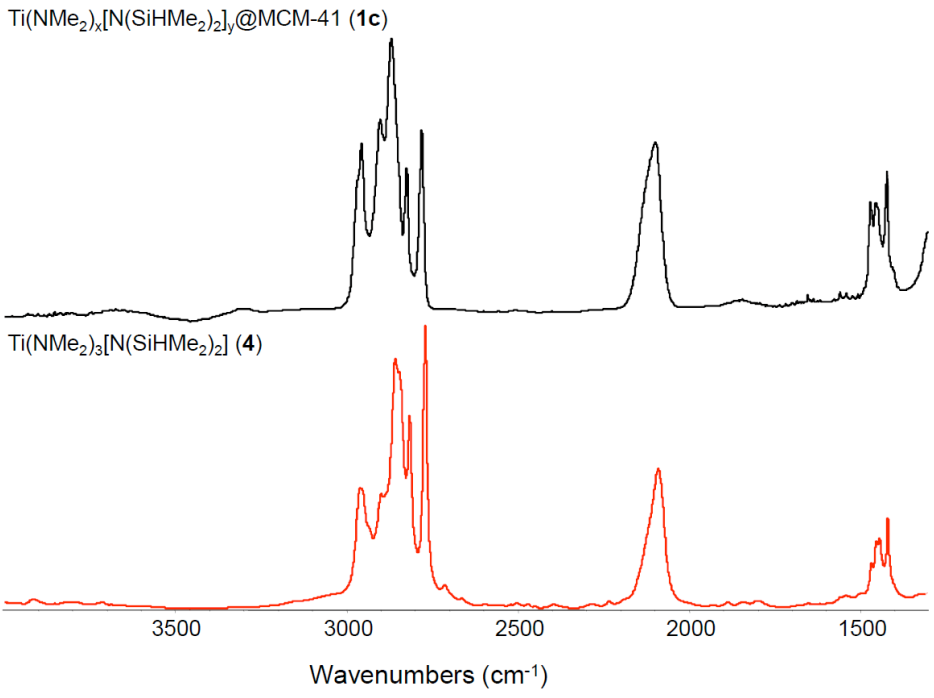

Figure S7. IR spectra (DRIFT) of the hybrid materials $Ti(NMe_2)_3[N(SiHMe_2)_2]$@MCM-41 (**1c**) and precursor $Ti(NMe_2)_3[N(SiHMe_2)_2]$ (**4**) in the range of 1300-4000 cm^{-1}.

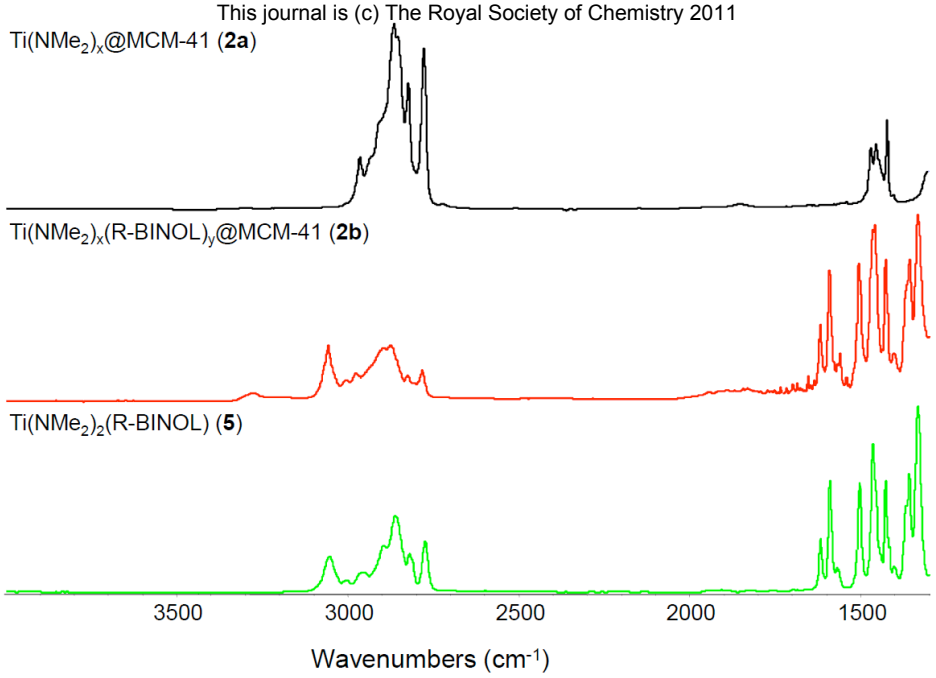

Figure S8. IR spectra (DRIFT) of the hybrid materials $Ti(NMe_2)_4$@MCM-41 (**2a**) and (*R*-H_2BINOL)@$Ti(NMe_2)_4$@MCM-41 (**2b**) and precursor $Ti(NMe_2)_2$(R-BINOL) (**5**) in the range of 1300-4000 cm^{-1}.

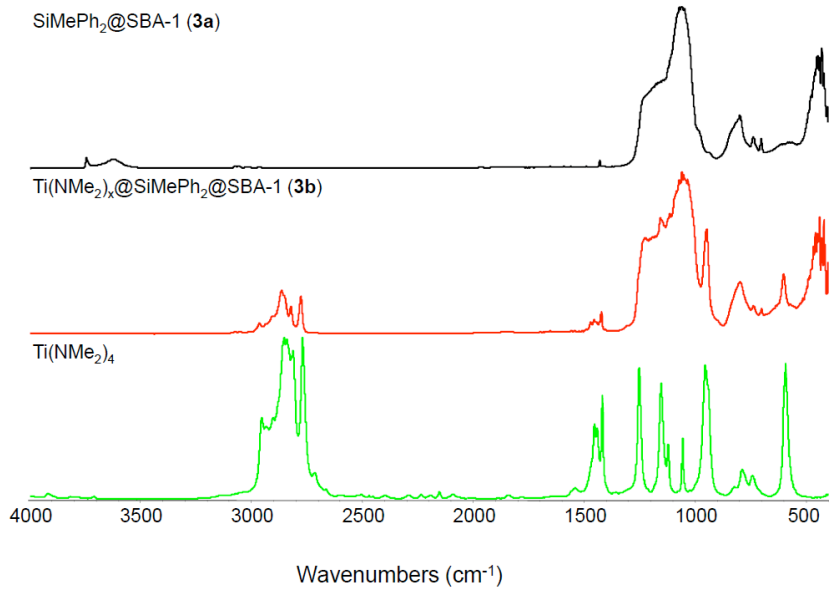

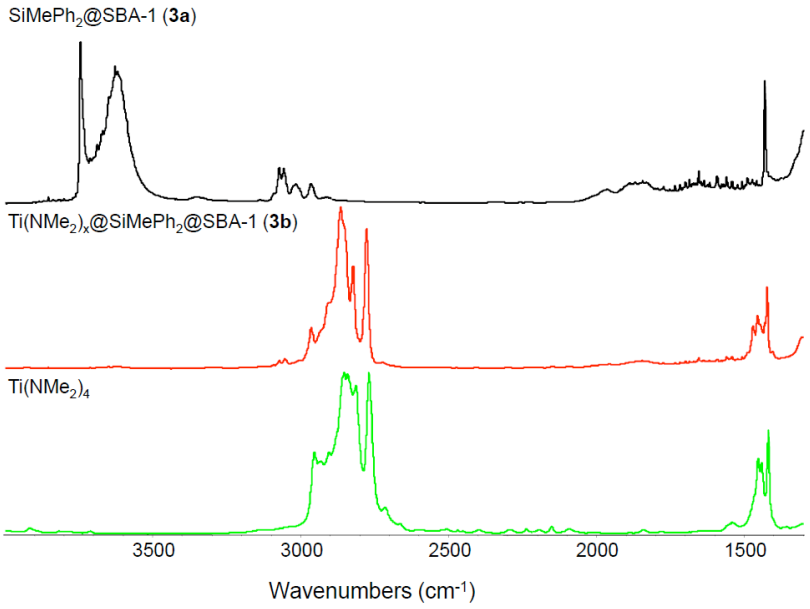

Figure S9. IR spectra (DRIFT) of the hybrid materials $SiMePh_2$@SBA-1 (**3a**) and $Ti(NMe_2)_4$@$SiMePh_2$@SBA-1 (**3b**) and precursor $Ti(NMe_2)_4$ in the range of 400-4000 cm^{-1} and 1300-4000 cm^{-1}.

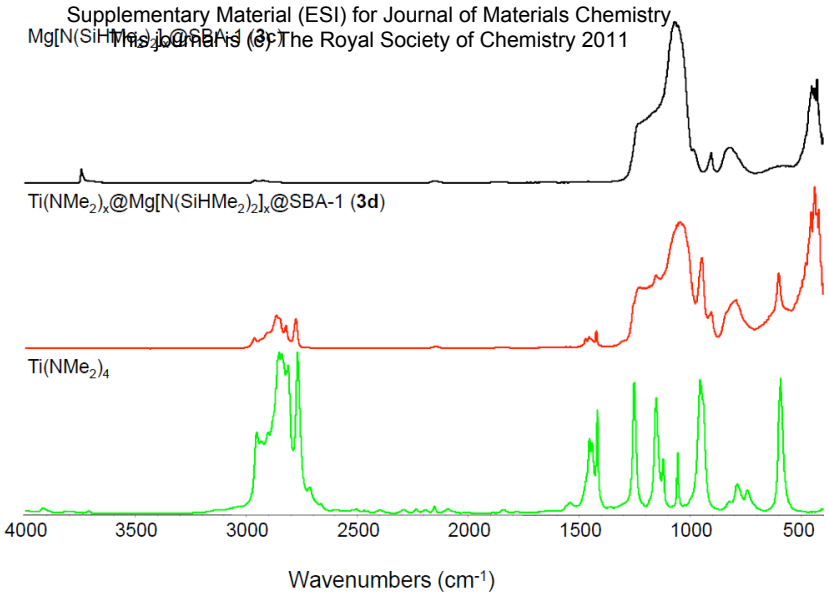

Figure S10. IR spectra (DRIFT) of the hybrid materials $Mg[N(SiHMe_2)_2]_2$@SBA-1 (**3c**) and $Ti(NMe_2)_4$@$Mg[N(SiHMe_2)_2]_2$@SBA-1 (**3d**) and precursor $Ti(NMe_2)_4$ in the range of 400-4000 cm^{-1}.

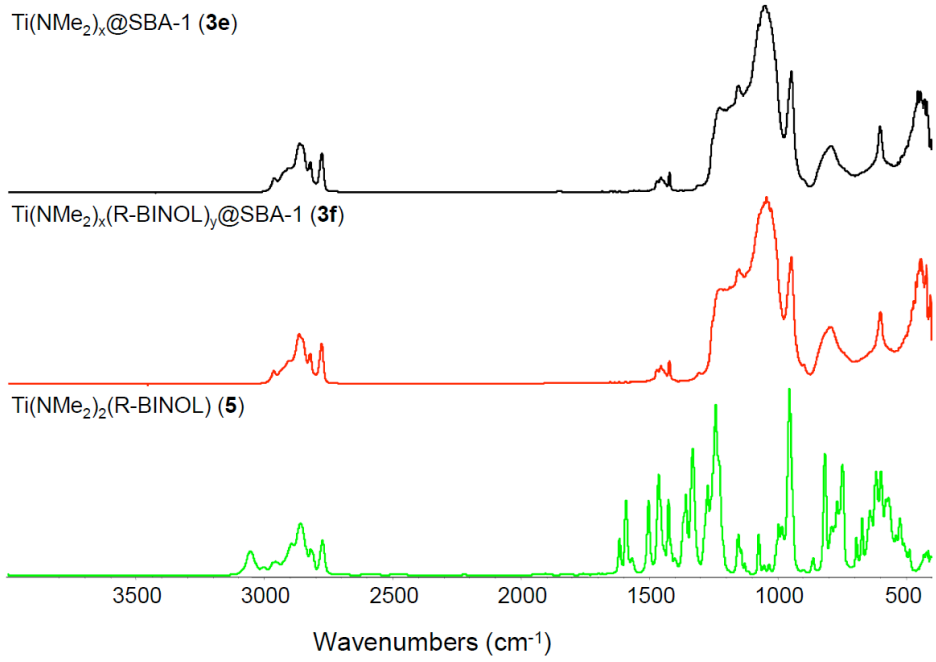

Figure S11. IR spectra (DRIFT) of the hybrid materials $Ti(NMe_2)_4$@SBA-1 (**3e**) and (R-H_2BINOL)@$Ti(NMe_2)_4$@ SBA-1 (**3f**) and precursor $Ti(NMe_2)_2$(R-BINOL) (**5**) in the range of 400-4000 cm^{-1}

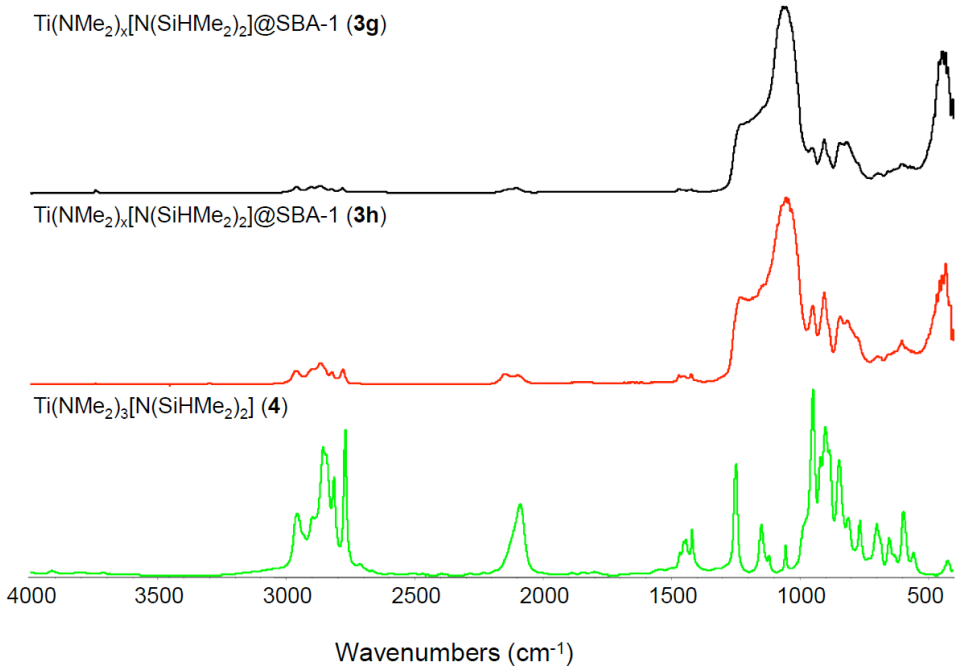

Figure S12. IR spectra (DRIFT) of the hybrid materials $Ti(NMe_2)_3[N(SiHMe_2)_2]$@SBA-1 (**3g**) and $Ti(NMe_2)_3[N(SiHMe_2)_2]$@SBA-1 (**3h**) and precursor $Ti(NMe_2)_3[N(SiHMe_2)_2]$ (**4**) in the range of 400-4000 cm^{-1}.

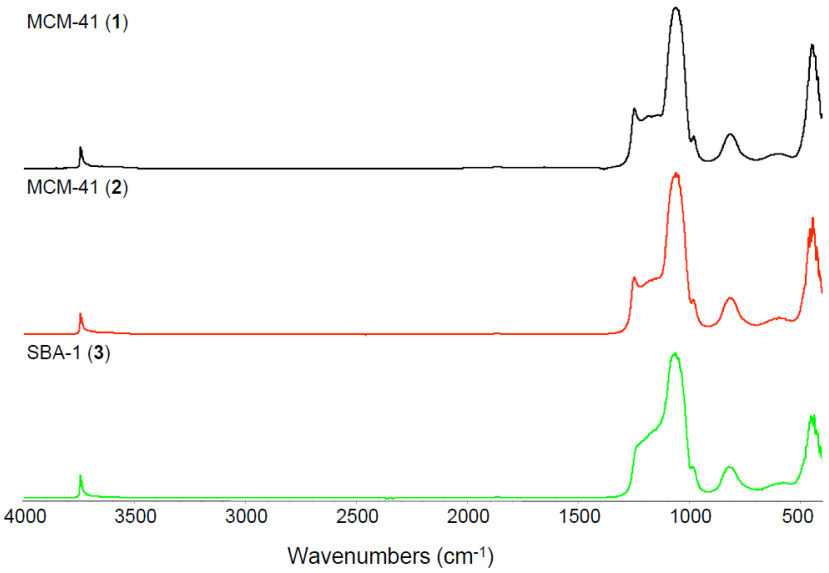

Figure S13. IR spectra (DRIFT) of the parent materials MCM-41 (**1**), MCM-41 (**2**) and SBA-1 (**3**) in the range of 400-4000 cm^{-1}.

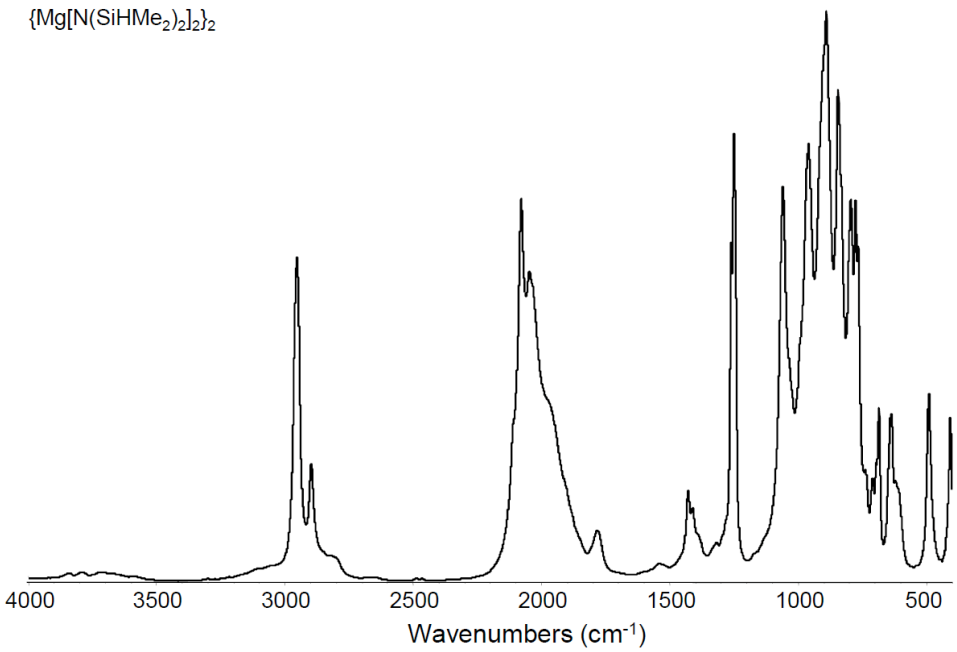

Figure S14. IR spectrum (DRIFT) of $\{Mg[N(SiHMe_2)_2]_2\}_2$ in the range of 400-4000 cm^{-1}.

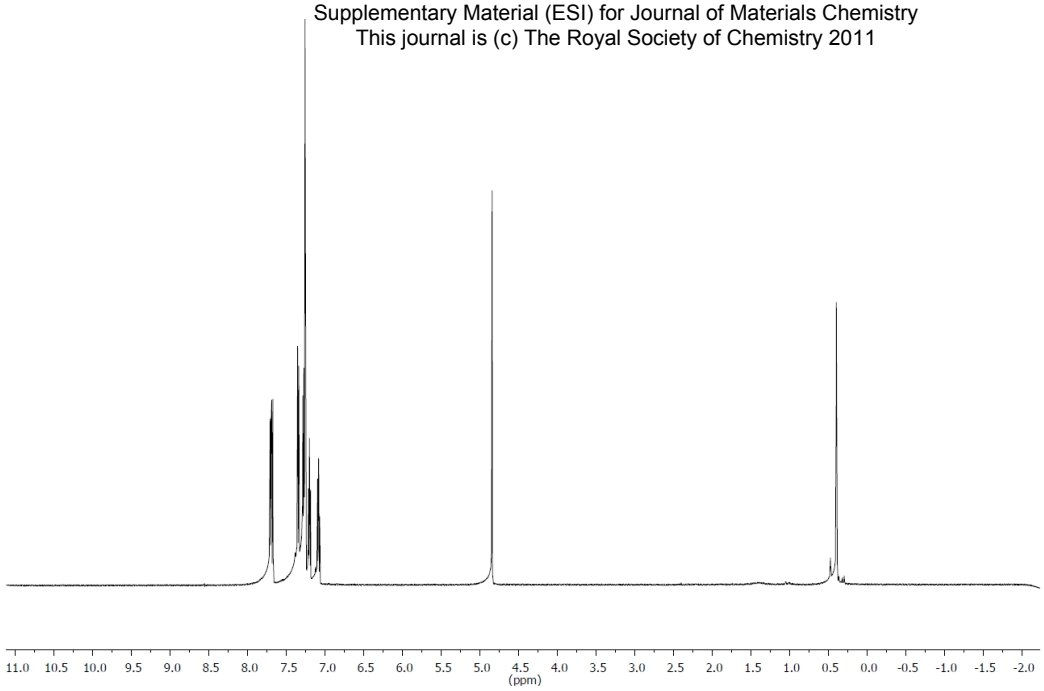

Figure S15. ^{1}H NMR spectrum (600.13 MHz) of *R*-H_2BINOL in C_6D_6.

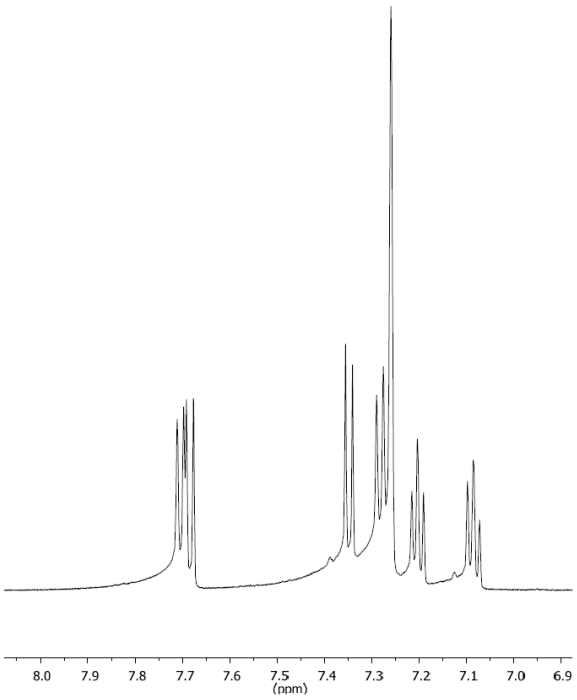

Figure S16. ^{1}H NMR spectrum (600.13 MHz) of *R*-H_2BINOL in C_6D_6.

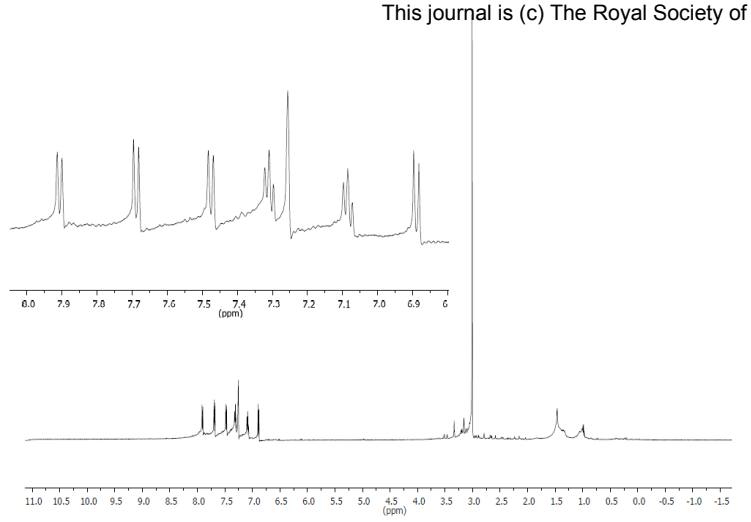

Figure S17. ^{1}H NMR spectrum (600.13 MHz) of Ti(NMe$_2$)$_2$(*R*-BINOL) (**5**) in C_6D_6.

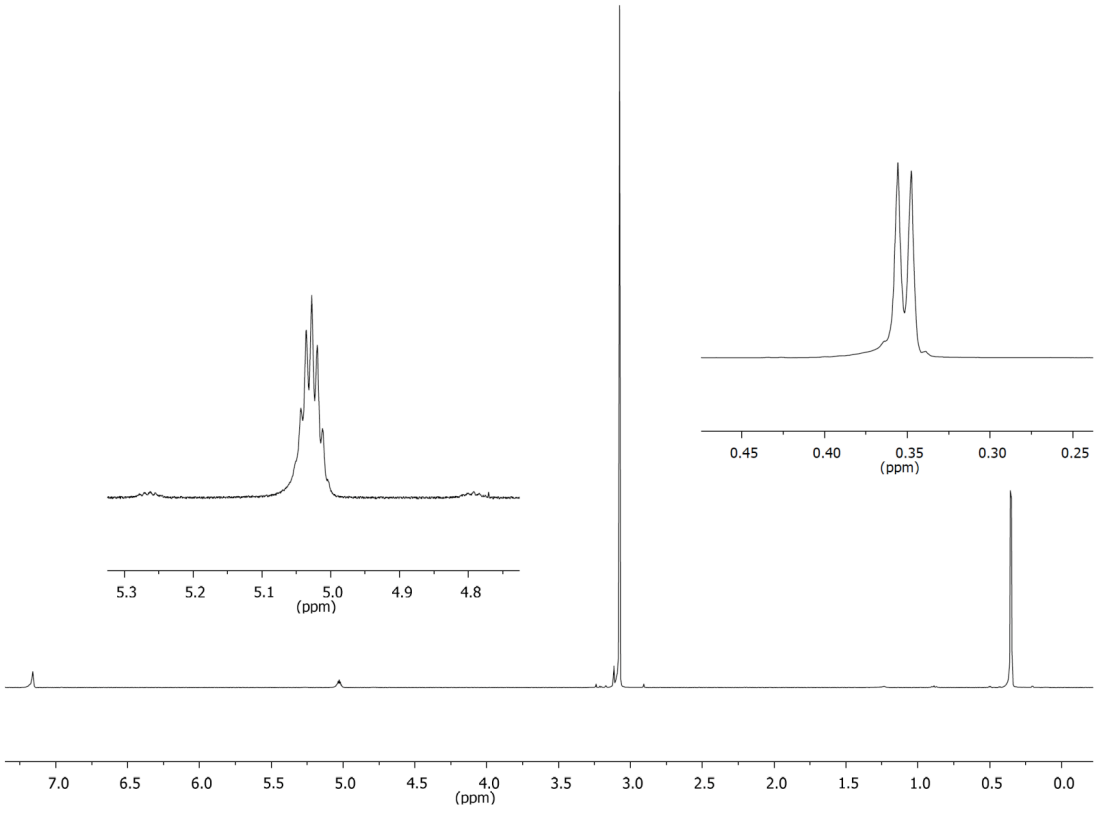

Figure S18. ^{1}H NMR spectrum (400.13 MHz) of Ti(NMe$_2$)$_3$[N(SiHMe$_2$)$_2$] (**4**) in C_6D_6.

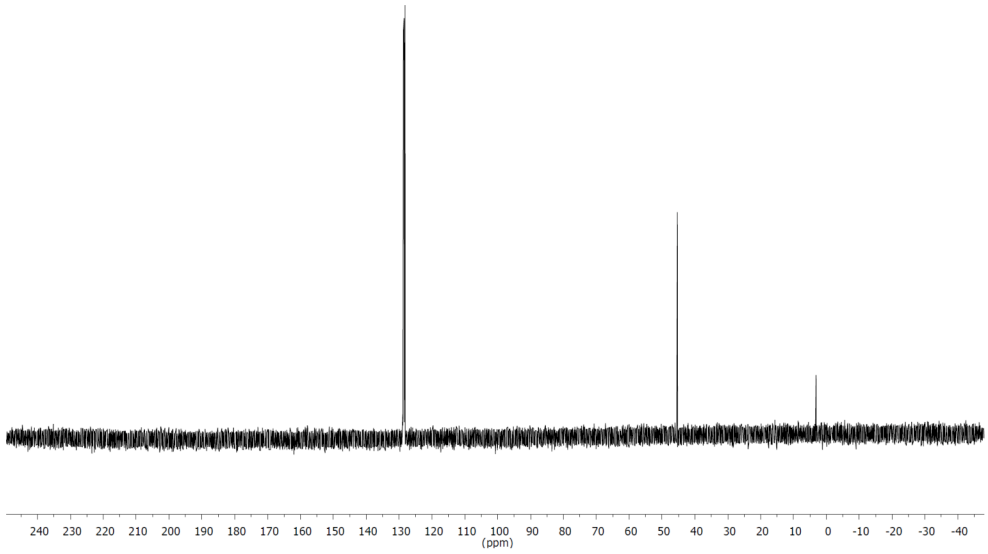

Figure S19. ^{13}C NMR spectrum (100.61 MHz) of $Ti(NMe_2)_3[N(SiHMe_2)_2]$ (**4**) in C_6D_6.

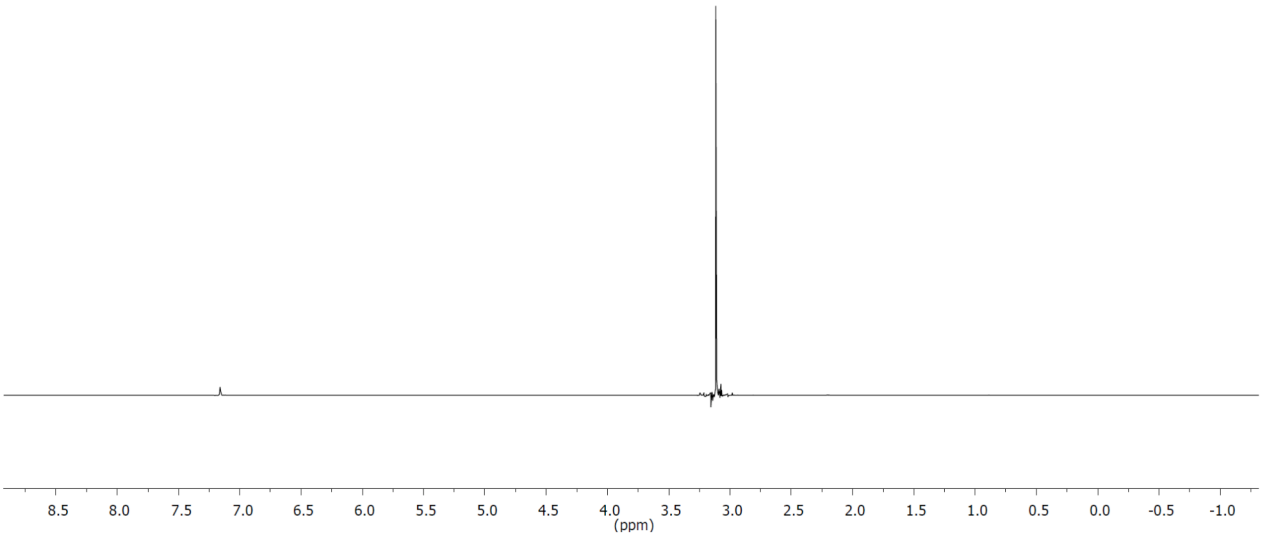

Figure S20. ^{1}H NMR spectrum (400.13 MHz) of $Ti(NMe_2)_4$ in C_6D_6.

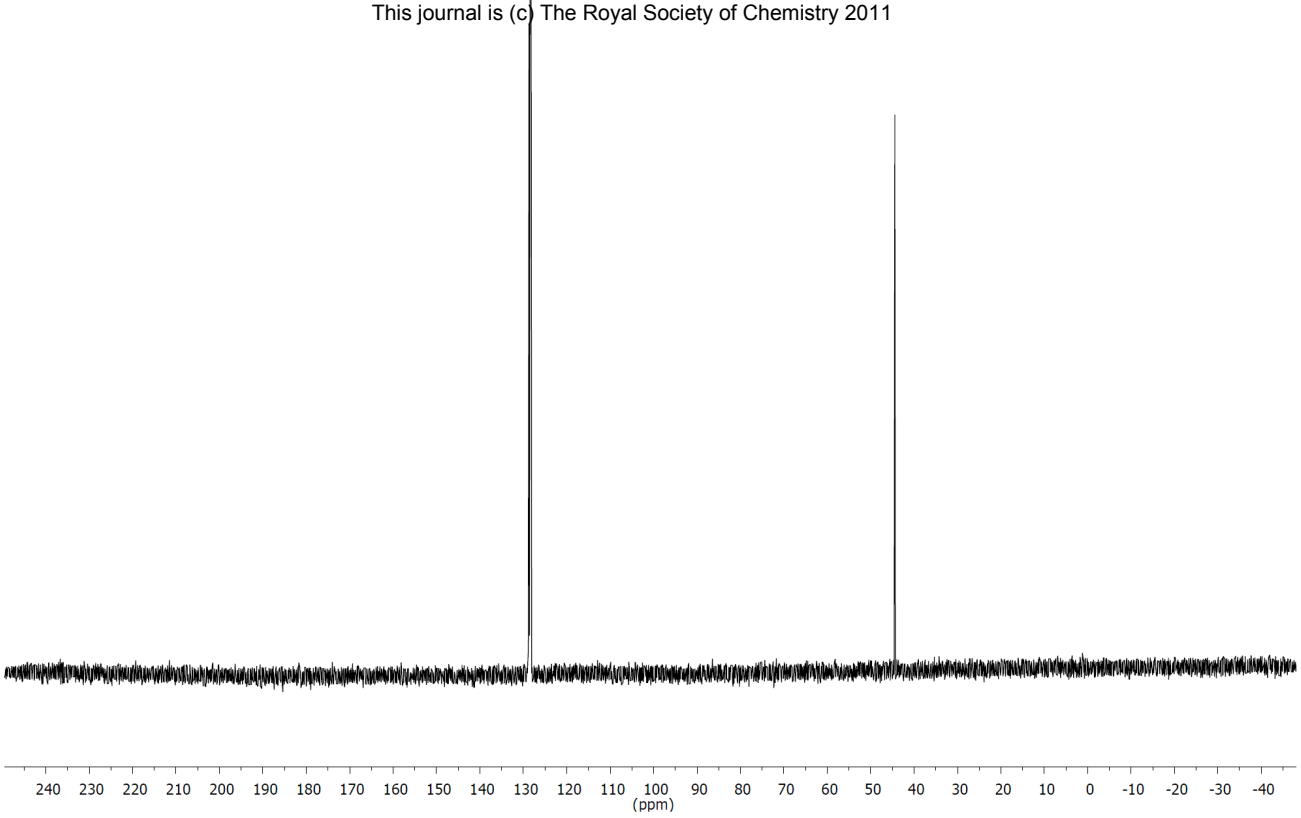

Figure S21. ^{13}C NMR spectrum (100.61 MHz) of $Ti(NMe_2)_4$ in C_6D_6.

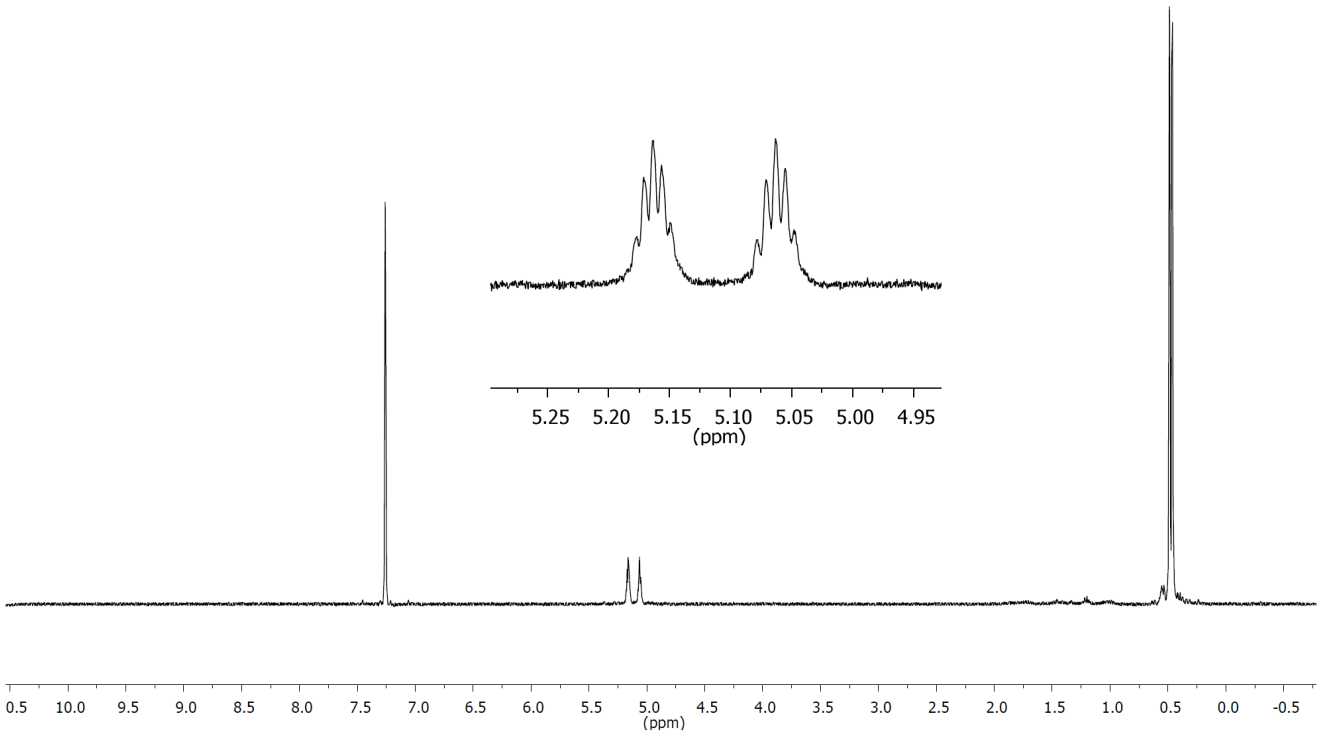

Figure S22. ^{1}H NMR spectrum (600.13 MHz) of $\{Mg[N(SiHMe_2)_2]_2\}_2$ in C_6D_6.

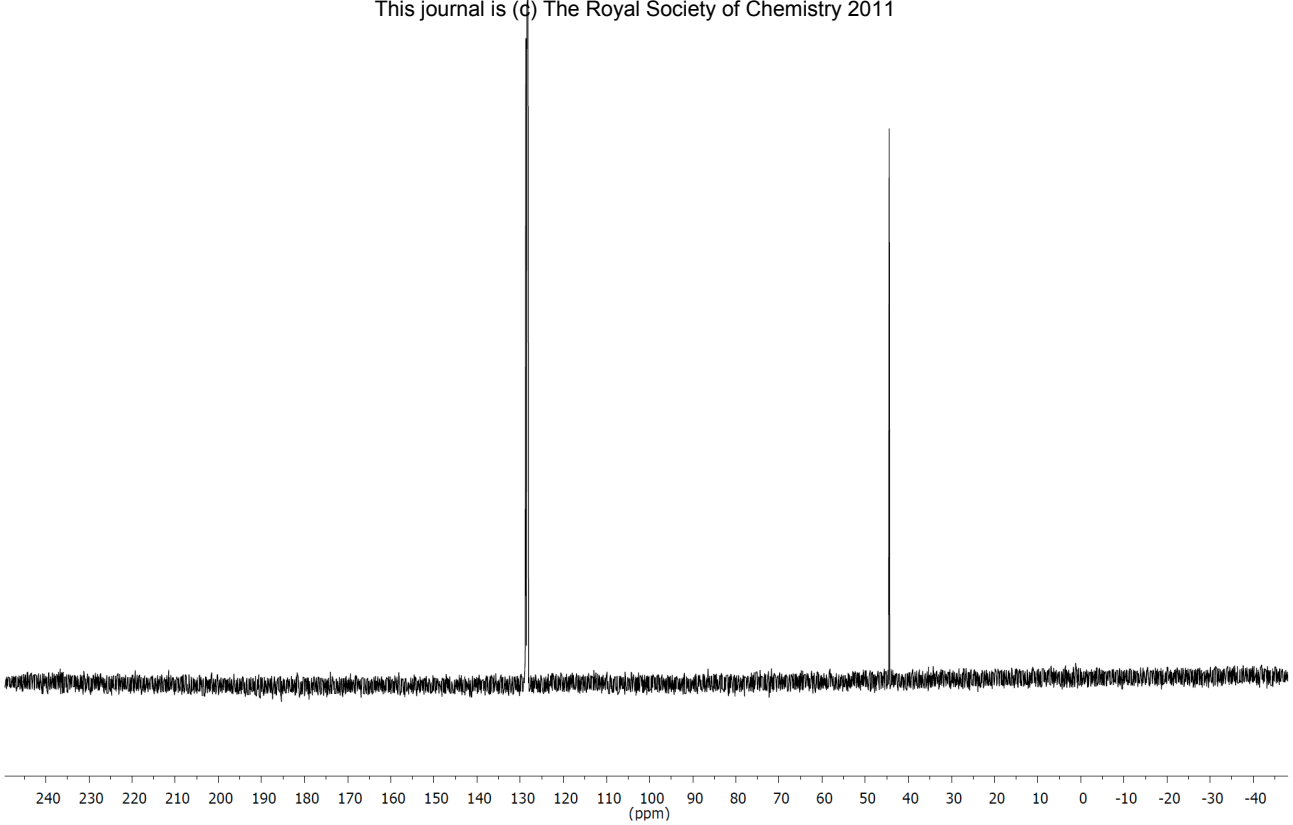

Figure S23. ^{13}C NMR spectrum (100.61 MHz) of $\{Mg[N(SiHMe_2)_2]_2\}_2$ in C_6D_6.